Article

Spray-Drying of Hydroxypropyl β-Cyclodextrin Microcapsules for Co-Encapsulation of Resveratrol and Piperine with Enhanced Solubility

Xing Yang [1,†]**, Jian Shen** [1,†]**, Jia Liu** [1]**, Yuxin Yang** [1]**, Anna Hu** [1]**, Na Ren** [2]**, Zeneng Cheng** [1] **and Wenjie Liu** [1,*]

[1] Xiangya School of Pharmaceutical Sciences, Central South University, Changsha 410013, China; 197211039@csu.edu.cn (X.Y.); 197211033@csu.edu.cn (J.S.); liujiayaoxue@csu.edu.cn (J.L.); 217211044@csu.edu.cn (Y.Y.); 217211048@csu.edu.cn (A.H.); chengzn@csu.edu.cn (Z.C.)

[2] Pharmaceutical Production Technology Teaching and Research Section, Hunan Vocational College of Science and Technology, Changsha 410004, China; rennaa@163.com

[*] Correspondence: wenjie.liu@csu.edu.cn; Tel.: +86-186-8466-8959

[†] These authors contributed equally to this work.

Abstract: The synergistic therapeutic benefits of resveratrol (RES) and piperine (PIP) have been proven for the treatment of various diseases. This study reports, for the first time, spray-drying of hydroxypropyl β-cyclodextrin (HP-β-CD) microcapsules for combined delivery of resveratrol and piperine. Phase solubility studies indicated that there was a strong interaction between the active ingredients and HP-β-CD, and both active ingredients can bind stably to HP-β-CD. The results of FTIR, XRD, and DSC demonstrated that RES-PIP/HP-β-CD inclusion complexes were successfully formed, with the RES and PIP encapsulated into the hollow spherical cavity of HP-β-CD. The results of SEM showed that the spray-dried microcapsules displayed a smooth surface and uniform particle size. Upon the formation of the spray-dried microcapsules, both RES and PIP presented significantly enhanced solubility. The results of DPPH and ABTS⁺ scavenging activity assays showed that the spray-drying process did not adversely influence the antioxidant activity of the bioactives, and the addition of PIP increased the antioxidation performance of RES.

1. Introduction

The consumption of functional food products or dietary supplements fortified with bioactive substances is gaining popularity due to increased awareness of consumers for imparting health benefits [1]. Co-encapsulation and simultaneous delivery of multiple bioactive substances in a single-wall system has been regarded as a novel approach for the development of health products with synergistic effects. Resveratrol (RES), a natural non-flavonoid polyphenol compound, is widely presented in natural plants such as grapes, strawberries, peanuts, knotweed, mulberry, etc. The earliest attention to RES is related to the interesting phenomenon of the "French Paradox". Although the French consume a high-fat diet, the incidence of cardiovascular disease is relatively low [2]. So far, RES has been reported to have various pharmacological effects, such as anti-cancer [3], anti-inflammatory, antioxidant [4,5], and cardiovascular protection [6]. It is probably the most common phytoalexin that has both been used in traditional medicine and explored in modern healthcare. However, the poor aqueous solubility, instability, and rapid metabolism of RES has significantly limited the efficacy of its therapeutic benefits.

Different approaches have been reported for enhancing the oral bioavailability of RES, such as micelles [7], solid dispersions [8], nanoparticles [9], and nano-emulsions [10]. Piperine (PIP), an alkaloid compound and the main active component of black pepper, has been disclosed, which could enhance the bioavailability of many pharmaceutical

ingredients through various proposed mechanisms, such as the inhibitory action on various hepatic and other metabolizing enzymes. Johnson et al. reported that with the addition of PIP, the in vivo exposure and maximum serum concentration of RES were increased to 229% and 1544%, respectively [11]. Jadhav et al. reported that the oral bioavailability of RES was increased by 5.7-fold when delivered by PIP-loaded mixed micelles [12]. Wightman et al. reported that co-supplementation of PIP with RES enhanced the bioefficacy of RES with regard to the increase of cerebral blood flow [13]. Meanwhile, pharmacological studies have shown that PIP presents potential therapeutic effects, such as anti-inflammatory [14], cytoprotective effects [15], and antioxidant [16]. The codelivery of PIP with RES would be a promising method to improve the bioperformance of RES with synergistic beneficial effects.

Even though PIP possesses bioenhancer properties, the solubility and dissolution behaviors of the co-encapsulated bioactive substances have important impacts on the absorption of RES. He et al. reported that unfavorable bioavailability of RES was observed for RES and PIP cocrystals due to the reduced dissolution and apparent solubility of the bioactive substances [17]. Therefore, it is necessary to develop a co-encapsulation technology to achieve solubilization of the bioactive substances. Improving the solubility of bioactive ingredients by preparing an inclusion complex has become a promising technology [18,19]. Cyclodextrin (CD) is a cyclic oligosaccharide derived from starch. The outer surface of CDs is hydrophilic, while the inner cavity is hydrophobic, which can accommodate insoluble molecules [20]. Hydrophobic β-cyclodextrin (HP-β-CD) is one of the most widely used CDs because its cavity is compatible with common guests and with high safety [21,22].

The aim of this study is to improve the solubility of RES and PIP by preparing an inclusion complex with HP-β-CD through spray-drying. To the best of our knowledge, this is the first study on co-encapsulation of RES and PIP via the spray-drying technique. As a powder production method commonly used in food and pharmaceutical fields, spray-drying possesses the advantages of being rapid, low-cost, and easily scalable [23,24]. Phase solubility studies were performed to evaluate the stability of RES and PIP in HP-β-CD. The complexes were characterized by various analytical techniques to confirm their formation. The structural and thermal properties of the spray-dried microcapsules were analyzed by Fourier transform infrared spectroscopy (FITR), X-ray diffraction (XRD), differential scanning calorimetry (DSC), and scanning electron microscopy (SEM). The antioxidant capacity of RES was evaluated by measuring the clearance of 1,1-diphenyl-2-picrylhydrazyl (DPPH) and 2,2'-Azinobis-3-ethylbenzthiazoline-6-sulphonate (ABTS). Furthermore, the water solubility of the inclusion complexes was assessed to verify the solubility enhancement of RES and PIP.

2. Materials and Methods

2.1. Materials

RES (99%), PIP (97%), ABTS (97%), and HP-β-CD (97%) were purchased from Aladdin (Shanghai, China). DPPH (98%) was purchased from Ryon (Shanghai, China). Hydrochloric acid, anhydrous ethyl alcohol, sodium hydroxide, and potassium dihydrogen phosphate of analytical grade were purchased from Sinopharm Chemical Reagent Co., Ltd. (Shanghai, China). Acetonitrile of HPLC grade was obtained from Merck Co., Ltd. (Waldbronn, Germany). Distilled water was used in all experimental procedures, which was provided by a laboratory water purification system (Hitech Instruments Co., Ltd., Shanghai, China).

2.2. Methods

2.2.1. Analysis of RES and PIP Contents by HPLC

HPLC analysis of the content of RES and PIP is based on the methodology of Kurang [25], with slight changes, using an Agilent 1200 system (Agilent Technologies, Waldbronn, Germany) with a UV-Vis detector. A reversed phase column (Agilent, C18, 4.6 × 250 mm) placed in a column oven was used for chromatographic separation at a constant flow rate of 1 mL/min, with a sample volume of 20 μL. RES and PIP were detected at the UV absorp-

tion wavelengths of 307 and 343 nm, respectively. The mobile phase used for RES analysis was acetonitrile:water (37:63, v/v) and the mobile phase used for PIP was acetonitrile:water (55:45, v/v). All samples were filtered through a 0.45 μm microporous membrane filter before injection.

2.2.2. Phase Solubility Study

Phase solubility studies were performed using the method described by Higuchi and Connors [26]. An excess amount of RES and PIP was added to 10 mL of deionized water with increasing HP-β-CD concentrations (ranging from 0 to 10 mM/L). The mixture was well-mixed by a magnetic agitator, and then shaken in the oscillator at 25 °C for 24 h. After equilibrium was reached, the mixture was filtered through a 0.45 μm microporous membrane, and the content of RES or PIP was measured using the quantitative HPLC analysis method established in Section 2.2.1. The experiment was performed in triplicate. The phase solubility diagrams were obtained by plotting between RES or PIP solubility and HP-β-CD concentrations. The stability constant (K_s) was calculated from the phase solubility diagram according to the following equation:

$$K_s = \text{Slope}/[S_0(1 - \text{Slope})] \tag{1}$$

where S_0 is the intrinsic solubility of RES or PIP in the absence of HP-β-CD and the Slope is the corresponding slope of the phase solubility diagram.

2.2.3. Spray-Drying of HP-β-CD Microcapsules

The compositions of feed solution for spray-drying are listed in Table 1. The mass ratio of RES to PIP in the formulations was fixed at 10:1, as used by Johnson et al. [11]. For the preparation of feed solution (a total volume of 250 mL), specific amounts of RES and PIP were dissolved in 15 mL of anhydrous ethanol, then added into the continuously stirred HP-β-CD solution in certain concentrations. The inclusion was carried out for a certain time period and spray-dried under specific inlet temperatures (Spray-dryer, MDSD-MARK III, Nantong Dong-Concept New Material Technology Co., Ltd., Nantong, China). The orifice diameter of the nozzle used for atomization was 100 μm and the hot air flow rate was kept at 250 L/min.

Table 1. Formulations of the feed solutions and process parameters used for spray-drying.

Sample No.	RES (g)	PIP (g)	HP-β-CD (g)	Inlet Temp. (°C)	Inclusion Time (min)	Drug Loading Efficiency (%)	
						RES	PIP
F1	2	0.2	4	180	30	32.2 ± 1.4	3.2 ± 0.1
F2	2	0.2	4	180	60	31.5 ± 1.5	3.1 ± 0.1
F3	2	0.2	4	180	120	31.2 ± 1.6	3.2 ± 0.3
F4	1	0.1	4	150	30	20.3 ± 1.2	2.0 ± 0.1
F5	1	0.1	4	180	30	18.7 ± 0.2	1.9 ± 0.1
F6	1	0.1	4	210	30	19.9 ± 1.4	1.9 ± 0.4
F7	1	0.1	7	180	30	12.7 ± 0.5	1.2 ± 0.1

2.2.4. Differential Scanning Calorimetry (DSC)

Differential scanning calorimetry (TG Technology, Q2000, New Castle, DE, USA) was carried out on representative samples. The 2–3 mg samples were placed in an aluminum disk, sealed, and put into the DSC detector. The test was conducted under a dynamic nitrogen atmosphere over the temperature range from 25 to 200 °C with a heating rate of 10 °C/min.

2.2.5. Particle Size Measurement

The mean diameter and particle size distribution of spray-dried microcapsules were evaluated by a laser diffraction particle size analyzer, using Partica LA-960V2 with the Wet Dispersion Unit module (Horiba, Kyoto, Japan).

2.2.6. Fourier Transform Infrared Spectroscopy (FTIR)

FTIR spectra of representative samples were measured using a FTIR spectrophotometer (Shimadzu, Tokyo, Japan, IRTracer-100). First, the sample was uniformly dispersed in KBr, and then the mixture was converted into a tablet using the KBr press. The tablet was placed in the sample stand of the FTIR spectrophotometer and scanned at a resolution of 2 cm^{-1} in the range of 400–4000 cm^{-1}.

2.2.7. X-ray Diffraction (XRD)

The X-ray diffraction patterns were obtained at room temperature by the Rigaku ultima 4 type polycrystalline powder X-ray diffractometer with CuKα radiation (Japan). All samples were analyzed in the 2θ angle range of 5–$90°$ at a rate of $1°/\text{min}$.

2.2.8. Scanning Electron Microscopy (SEM)

The spray-dried samples were placed on carbon tapes on aluminum sample slabs and made electrically conductive by sputtering with a thin layer of gold for 80 s prior to analysis. The SEM images were acquired using a scanning electron microscope (JSM 7200F, JEOL, Tokyo, Japan) operating at an accelerating voltage of 10 kV.

2.2.9. Drug Loading Efficiency

The amount of RES and PIP encapsulated into the spray-dried microcapsules was quantified by dissolving an accurately weighted amount of sample in 10 mL of ethanol. After full dissolution of the microcapsules, the solutions were filtered through 0.45 μm microporous membranes prior to HPLC quantification. Drug loading efficiency (LE%) was calculated according to the following formula: Drug loading efficiency (%) = weight of RES or PIP in inclusion complex/weight of total inclusion complex $\times$ 100%. All analyses were performed in triplicate.

2.2.10. Characterization of Antioxidant Activity
DPPH Radical Scavenging Test

DPPH scavenging activity was evaluated using a modified method according to a previous study [27]. In brief, samples (raw RES or spray-dried microcapsules) were dissolved in ethanol to obtain a RES concentration of 0–100 μg/mL. Then, 1 mL of the sample solution was mixed with 1 mL of 250 μg/mL DPPH ethanol solution, and kept in the dark for 30 min. The resulting solution was centrifuged at $4000\times g$ for 5 min and the absorbance of the supernatant was measured at 517 nm using a UV-Vis spectroscope (UV-2600, Shimadzu, Tokyo, Japan. The solution without any sample was used as the control. The DPPH scavenging rate is expressed as the following equation:

$$\text{DPPH scavenging rate (\%)} = [1 - (\text{Sample}_{Abs}/\text{Control}_{Abs})] \times 100\% \qquad (2)$$

ABTS$^+$ Radical Scavenging Test

ABTS$^+$ radical scavenging activity was conducted following the reported method with some modifications [28]. The ABTS$^+$ working solution was prepared by mixing 7.5 mL of a 7 mM ABTS aqueous solution with 132 μL of a 140 mM $K_2S_2O_8$ solution. This mixture was kept in the dark for at least 12 h, and then was diluted with deionized water until it reached an absorbance of 0.7 ± 0.1 at 734 nm. The samples (raw RES or spray-dried microcapsules) were dissolved in ethanol to obtain a RES concentration of 0–500 μg/mL. Then, 10 μL of the sample solution was mixed with 500 μL of ABTS$^+$ working solution and the absorbance at 734 nm was determined after the reaction of avoiding light for 1 h. The solution without

any sample was used as the control. The ABTS$^+$ scavenging rate was calculated by the following equation:

$$\text{ABTS}^+ \text{ scavenging rate (\%)} = [1 - (\text{Sample}_{\text{Abs}}/\text{Control}_{\text{Abs}})] \times 100\% \tag{3}$$

2.2.11. Equilibrium Solubility

The equilibrium solubility of RES and PIP in raw form or in the spray-dried microcapsules were determined. An excess amount of sample was added to different media (pH 1.2 hydrochloric acid solution, pH 4.5 and pH 6.8 phosphate buffer, and water). The mixtures were stirred for 24 h at 37 °C. After equilibrium was reached, the mixture was filtered through a 0.45 µm microporous membrane, and the content of RES or PIP was measured using the quantitative HPLC analysis method established in Section 2.2.1. The experiment was performed in triplicate.

3. Results and Discussion

3.1. Phase Solubility

The phase solubility describes the solubilizing ability of the host molecules and the stability constant. The phase solubility behavior of RES and PIP in the HP-β-CD water solution at 37 °C was evaluated, respectively. The phase solubility curve showed that HP-β-CD has a good solubilization effect on both RES and PIP, and the concentrations of RES and PIP in the solution increased linearly with increasing HP-β-CD concentration (Figure 1). It can be classified as AL type as per the model proposed by Higuchi and Connors [29]. The increase in solubility can be caused by the formation of a water-soluble inclusion complex between the bioactive substances and HP-β-CD. The inclusion complex exhibits greater solubility than the pure bioactive substances, and the formed inclusion complexes are in 1:1 stoichiometry. The apparent stability constant (Ks) was calculated from the straight line of the phase solubility diagram as per the stability constant equation. The inclusion constant reflects the binding strength between the bioactive substances and HP-β-CD. The ideal range of the inclusion constant is 100–5000 Lmol^{-1} [30]. The inclusion constants of RES and PIP with HP-β-CD were 1861 and 591 Lmol^{-1}, respectively, indicating that there was a strong interaction between the bioactive substances and HP-β-CD. Both the bioactive substances could stably bind to HP-β-CD. The complex of RES with HP-β-CD has a higher value of inclusion constant than the complex of PIP, indicating that the permeation of the PIP into the macrocyclic cavity of the cyclodextrin may be less effective.
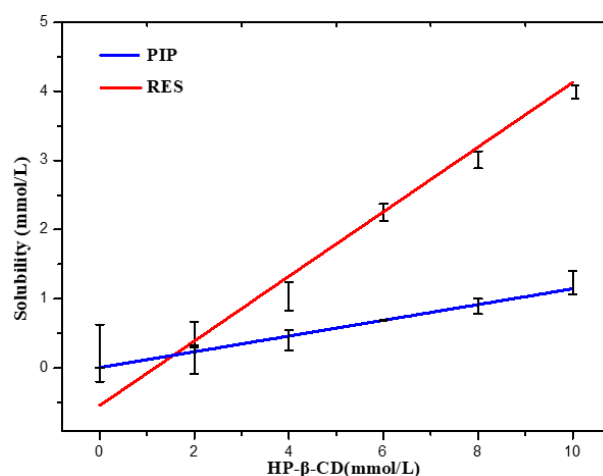

Figure 1. Phase solubility diagram of RES and PIP.

3.2. FTIR Analysis

FTIR was used to analyze the interaction between the bioactive substances and the carrier material. The FTIR spectra of RES, PIP, HP-β-CD, physical mixtures (mixture of RES,

PIP and HP-β-CD), and spray-dried microcapsules are presented in Figure 2. RES showed characteristic peaks at 3247.35 cm^{-1} (phenolic O-H), 1616.76 cm^{-1} (C=O), 1588.91 cm^{-1} (aromatic C=C), 825 and 1020 cm^{1} (C–H bond substituted on C=C), and 1148.00 cm^{-1} (C–O stretching) [31,32]. PIP showed characteristic peaks at 1659 cm^{-1} (CO–N stretching), 3011.3 cm^{-1} (aromatic C–H), and 1254.47 cm^{-1} (O–CH2–O stretching) [12,33]. HP-β-CD showed characteristic peaks at 3335.54 cm^{-1} (–OH stretching), 2915 cm^{-1} (for C–H stretching vibrations), 1630 cm^{-1} (for H–O–H bending), 1164 cm^{-1} (for C–O stretching vibrations), and 1028 cm^{-1} (for C–O–C stretching vibrations) [34]. The FTIR spectra of the physical mixtures did not significantly differ from those of the single components. However, bands of RES in spray-dried microcapsules, such as 1041, 1148.00, and 1588.91 cm^{-1}, were absent, whereas the new bands appeared at 1041.00, 1121.00, and 1610.93.cm^{-1}. The bands related to the PIP located at 1659.00 and 1254.47 cm^{-1} were shifted to 1625.00 and 1230.00 cm^{-1}. Some native bands of cyclodextrin (e.g., 2915 and 3335.54 cm^{-1}) were observed in the spectra of the inclusion complex, and this might be due to the formation of new chemical bonds with cyclodextrin.
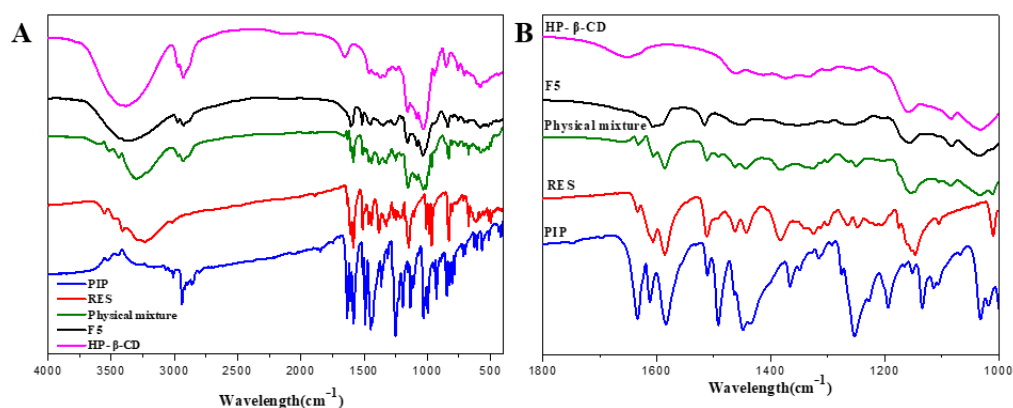
Figure 2. FTIR spectra of (**A**,**B**) RES, PIP, HP-β-CD, physical mixture, and representative spray-dried microcapsules (F5).

3.3. Morphological Characterization

Figure 3 shows the SEM images of the spray-dried microcapsules of different formulations. The microcapsules all displayed a spherical shape with smooth or wrinkled surfaces. Comparing Figure 3A,C,E, it can be seen that the surface of the microsphere becomes smoother with the decreasing core-wall ratio. By comparing Figure 3B–D, it was found that as the inlet temperature increases, the surface of the microcapsules becomes smoother. However, if the temperature is too high, the water loss (i.e., the drying rate) will be accelerated, causing the formed microspheres to rupture, or small pores to appear on the capsule wall, which may accelerate the deterioration of the encapsulated bioactives. The mean diameter of spray-dried microcapsules is depicted by the particle size measurement results in Figure 4. As shown in the figure, all the particle size distributions were of a normal distribution, indicating that the prepared microcapsules had a uniform particle size, which was consistent with the SEM observations.

3.4. XRD Analysis

The XRD profiles of RES, PIP, HP-β-CD, physical mixture (mixture of RES, PIP, and HP-β-CD), and representative spray-dried microcapsules (F5) are shown in Figure 5. Raw RES and PIP showed obvious characteristic diffraction peaks at 6.48°, 16.33°, 19.12°, and 28.34°, and 14.72°, 21.48°, 25.66°, and 28.23°, respectively, indicating their crystalline state. HP-β-CD displayed no obvious characteristic peak, indicating that the excipient itself was in an amorphous state. The XRD pattern of the physical mixture can be described as the overlap of the bioactive substances and HP-β-CD. For the spray-dried microcapsules, the characteristic diffraction peaks of RES and PIP all disappeared, suggesting that two

bioactive substances were transformed into an amorphous form upon the formation of microcapsules by spray-drying.
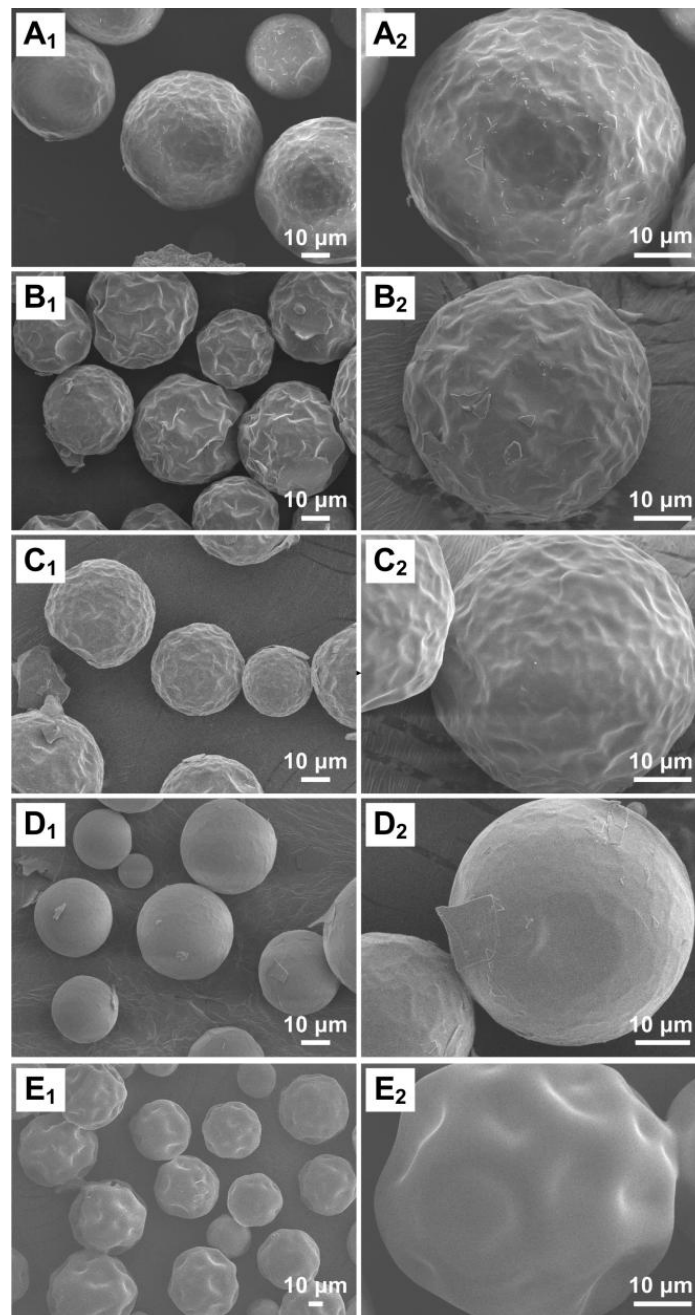
Figure 3. Scanning electron microscopy images of spray-dried microcapsules: (**A$_1$**,**A$_2$**): F1, (**B$_1$**,**B$_2$**): F4, (**C$_1$**,**C$_2$**): F5, (**D$_1$**,**D$_2$**): F6, and (**E$_1$**,**E$_2$**): F7.
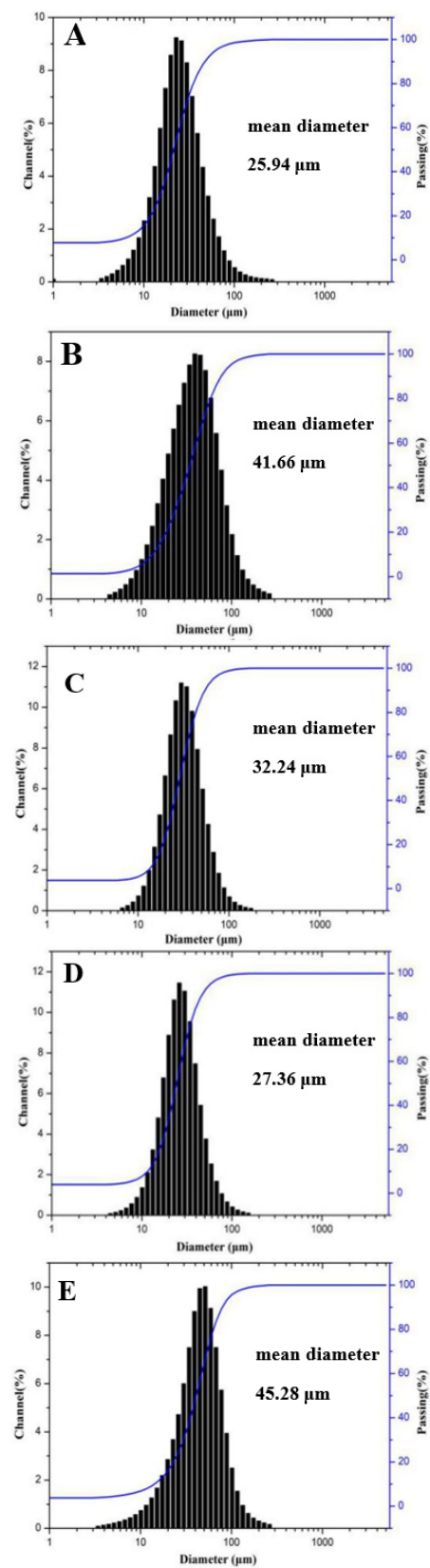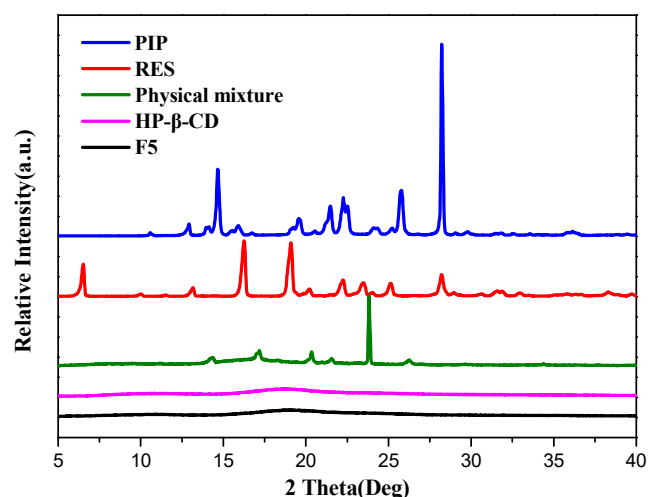
Figure 4. Size distribution of spray-dried microcapsules: (**A**) F1, (**B**) F4, (**C**) F5, (**D**) F6, and (**E**) F7.

Figure 5. XRD profiles of RES, PIP, HP-β-CD, physical mixture, and representative spray-dried microcapsules (F5).

3.5. DSC Analysis

DSC analysis was used to confirm the formation of the inclusion complexes in the solid state. The disappearance of the thermal peak of the guest molecule after inclusion can indicate the successful preparation of the inclusion complex. The DSC profiles of RES and PIP showed sharp endothermic peaks at 268.51 and 207.05 °C, respectively (Figure 6). The physical mixture displayed the sum thermogram peaks of two free components, which indicated that free RES/PIP and HP-β-CD did not interact with each other. Based on the curves of F5, the endothermic peaks of RES and PIP completely disappeared. This phenomenon could be caused by the encapsulation of both RES and PIP into the cylindrical cavity of HP-β-CD, and thus the thermal properties of the host and guest molecules were changed.
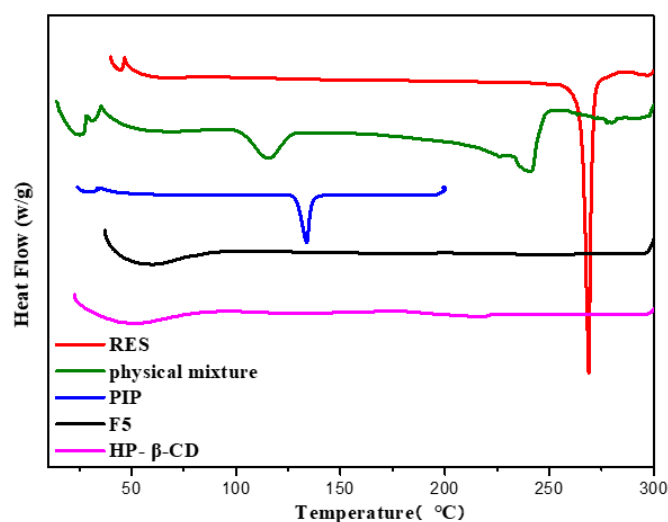

Figure 6. DSC profiles of RES, PIP, HP-β-CD, physical mixture, and representative spray-dried microcapsules (F5).

3.6. Equilibrium Solubility Study

The equilibrium solubility of RES and PIP in the spray-dried microcapsules was evaluated by preparing saturated solutions in different media. As can be seen from Figure 7, the solubility of RES and PIP in the spray-dried microcapsules in all media was higher than that of the raw substances, and the solubility increased with the increase of the ratio of HP-β-CD. When the mass ratio of HP-β-CD to RES was 7:1, RES and PIP exhibited

the best solubilization effect. The solubility of RES in water increased by approximately 18 times, from 39.73 to 724.49 µg/mL, and meanwhile the solubility of PIP increased by approximately 26 times, from 6.88 to 179.65 µg/mL for the sample of F7. Since the outer surface of HP-β-CD is hydrophilic while the inner cavity of HP-β-CD is hydrophobic, hydrophobic bioactive substances (RES and PIP in this study) could be accommodated into the inner cavity and interact with HP-β-CD by intermolecular hydrogen bonds. Therefore, the solubility of RES and PIP was significantly improved by using HP-β-CD as encapsulation wall material. The higher the proportion of HP-β-CD, the more bioactive substances may be encapsulated, and the solubilization effect would be better. However, if the proportion of the HP-β-CD ratio is too high, the drug loading will decrease, which is not conducive to practical applications. In this study, although F7 showed the best solubilization effect, the drug loading was relatively low. When the mass ratio of HP-β-CD to RES was 4:1, the solubility of RES and PIP in water also increased by about 21 and 16 times, respectively. Thus, F5 was selected to comprehensively carry out the antioxidant study, considering the drug loading and improved solubility.
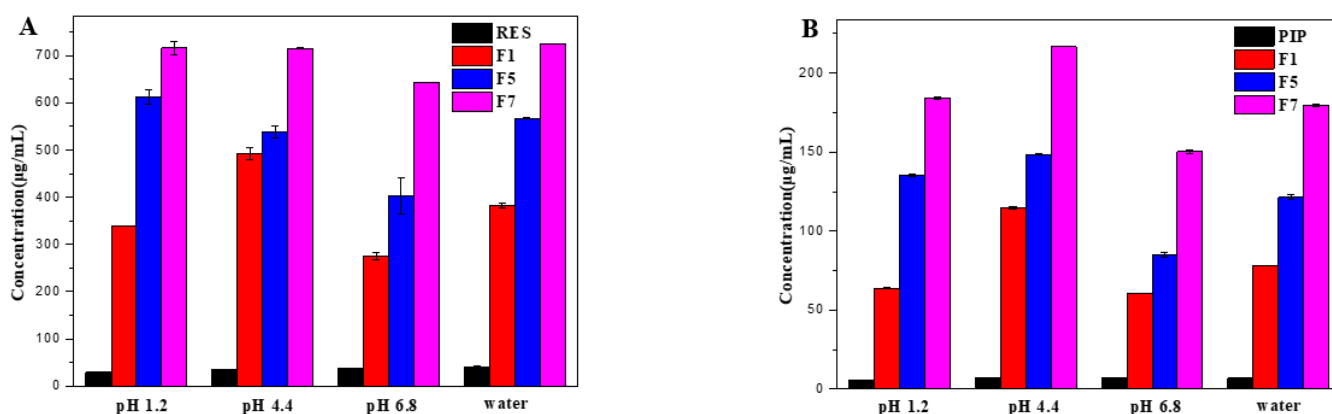
Figure 7. Equilibrium concentrations of RES (**A**), PIP (**B**), and the representative spray-dried microcapsules (F1, F5, and F7) in different media.

3.7. Antioxidant Capacity

The scavenging ability of DPPH free radical and ABTS+ were used to evaluate the synergistic effect of PIP on the antioxidant activity of RES. DPPH is a stable free radical, which can form a dark purple solution in organic solvents. When antioxidants are present, the ultraviolet absorption of DPPH in 517 nm will change. ABTS+ are generated in the presence of peroxides, used to determine the total antioxidant activity of substances in the solution [35]. The results (Figure 8) indicated that along with the increased concentration of RES, the DPPH scavenging capacities of both samples increased, and the PIP also exhibited a certain antioxidant capacity. Besides, the antioxidant capacity of microcapsules was higher than that of free RES at the same concentration. The ABTS+ scavenging ability of the microcapsules was also stronger than that of free RES. This may be the result of the effective protection property of the HP-β-CD cavity, which protects the antioxidation of RES during spray-drying, and the synergistic effect of PIP for the increase in the antioxidant properties.
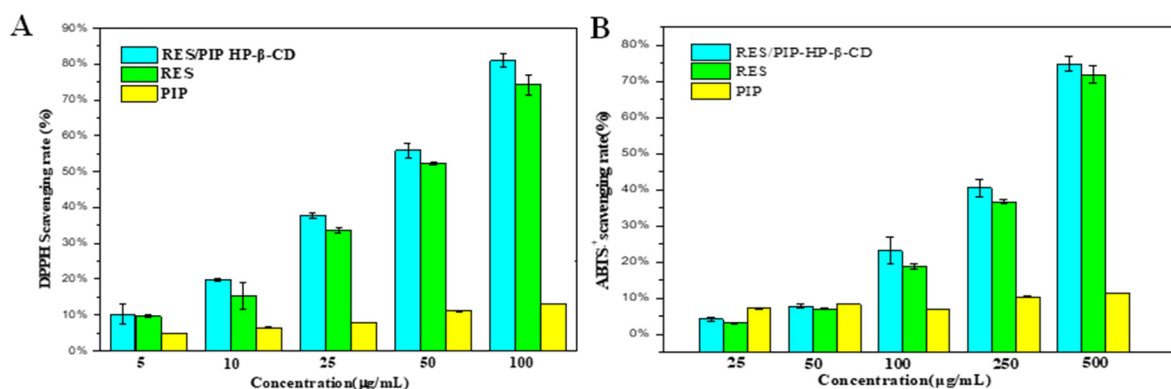
Figure 8. (**A**) DPPH scavenging rate of raw RES, raw PIP, and RES/PIP-HP-β-CD. (**B**) ABTS⁺ radical scavenging rate of raw RES, raw PIP, and RES/PIP-HP-β-CD.

4. Conclusions

This study has revealed that RES and PIP can be efficaciously co-entrapped by HP-β-CD as wall material via the spray-drying technique. The microcapsules of RES and PIP with HP-β-CD were prepared and investigated. Phase solubility studies indicated that there was a strong interaction between the bioactive substances and HP-β-CD, and both bioactive substances could stably bind to HP-β-CD. The results of FTIR, XRD, and DSC demonstrated that the RES-PIP/HP-β-CD inclusion complexes were successfully formed, with the RES and PIP encapsulated into the inner cavity of HP-β-CD. SEM observation showed that the spray-dried microcapsules were of spherical shape and uniform particle size. After the formation of the inclusion complexes, the solubility of RES and PIP was significantly enhanced. The results of DPPH and ABTS+ scavenging tests showed that the co-encapsulation of PIP increased the antioxidation performance of RES. The findings would be useful for the promotion of innovative food products with multiple bioactive compounds.

Author Contributions: Methodology, Investigation, Writing—original draft, writing—review & editing, X.Y.; writing—original draft, methodology, J.S.; data curation, J.L.; formal analysis, conceptualization, Y.Y.; investigation, project administration, A.H.; data curation, formal analysis, N.R.; supervision, Z.C.; conceptualization, writing—review & editing, W.L. All authors have read and agreed to the published version of the manuscript.

Data Availability Statement: The data presented in this study are available in reference [12,31,32,34,35].

Conflicts of Interest: The authors declare no conflict of interest.

Abbreviations

RES	Resveratrol
PIP	Piperine
HP-β-CD	Hydroxypropyl β-cyclodextrin
DPPH	1,1-diphenyl-2-picrylhydrazyl
ABTS	2,2′-Azinobis-(3-ethylbenzthiazoline-6-sulphonate)
FTIR	Fourier transform infrared spectroscopy
XRD	X-ray diffraction
DSC	Differential scanning calorimetry
SEM	Scanning electron microscopy
HPLC	High-performance liquid chromatography

References

1. Banwo, K.; Olojede, A.O.; Adesulu-Dahunsi, A. Functional importance of bioactive compounds of foods with Potential Health Benefits: A review on recent trends. *Food Biosci.* **2021**, *43*, 101320. [CrossRef]
2. Renaud, S.; Lorgeril de, M. Wine, alcohol, platelets, and the French paradox for coronary heart disease. *Lancet* **1992**, *339*, 1523–1526. [CrossRef]
3. Bian, P.; Hu, W.; Liu, C. Resveratrol potentiates the anti-tumor effects of rapamycin in papillary thyroid cancer: PI3K/AKT/mTOR pathway involved. *Arch. Biochem. Biophys.* **2020**, *689*, 108461. [CrossRef]
4. Recalde, M.D.; Miguel, C.A.; Noya-Riobo, M.V. Resveratrol exerts anti-oxidant and anti-inflammatory actions and prevents oxaliplatin-induced mechanical and thermal allodynia. *Brain Res.* **2020**, *1748*, 147079. [CrossRef]
5. Abbas, H.; Kamel, R.; El-Sayed, N. Dermal anti-oxidant, anti-inflammatory and anti-aging effects of Compritol ATO-based Resveratrol colloidal carriers prepared using mixed surfactants. *Int. J. Pharm.* **2018**, *541*, 37–47. [CrossRef]
6. Bhullar, K.S.; Udenigwe, C.C. Clinical evidence of resveratrol bioactivity in cardiovascular disease. *Curr. Opin. Food Sci.* **2016**, *8*, 68–73. [CrossRef]
7. Cheng, H.; Dong, H.; Liang, L. A comparison of beta-casein complexes and micelles as vehicles for trans-/cis-resveratrol. *Food Chem.* **2020**, *330*, 127209. [CrossRef]
8. Vasconcelos, T.; Prezotti, F.; Araujo, F. Third-generation solid dispersion combining Soluplus and poloxamer 407 enhances the oral bioavailability of resveratrol. *Int. J. Pharm.* **2021**, *595*, 120245. [CrossRef] [PubMed]
9. Huang, X.; Liu, Y.; Zou, Y. Encapsulation of resveratrol in zein/pectin core-shell nanoparticles: Stability, bioaccessibility, and antioxidant capacity after simulated gastrointestinal digestion. *Food Hydrocoll.* **2019**, *93*, 261–269. [CrossRef]
10. Zhu, P.; He, J.; Huang, S. Encapsulation of resveratrol in zein-polyglycerol conjugate stabilized O/W nanoemulsions:Chemical stability, in vitro gastrointestinal digestion, and antioxidant activity. *LWT* **2021**, *149*, 112049. [CrossRef]
11. Johnson, J.J.; Nihal, M.; Siddiqui, I.A. Enhancing the bioavailability of resveratrol by combining it with piperine. *Mol. Nutr. Food Res.* **2011**, *55*, 1169–1176. [CrossRef] [PubMed]
12. Jadhav, P.; Bothiraja, C.; Pawar, A. Resveratrol-piperine loaded mixed micelles: Formulation, characterization, bioavailability, safety and in vitro anticancer activity. *RSC Adv.* **2016**, *6*, 112795–112805. [CrossRef]
13. Wightman, E.L.; Reay, J.L.; Haskell, C.F. Effects of resveratrol alone or in combination with piperine on cerebral blood flow parameters and cognitive performance in human subjects: A randomised, double-blind, placebo-controlled, cross-over investigation. *Br. J. Nutr.* **2014**, *112*, 203–213. [CrossRef] [PubMed]
14. Shrivastava, P.; Vaibhav, K.; Tabassum, R. Anti-apoptotic and anti-inflammatory effect of Piperine on 6-OHDA induced Parkinson's rat model. *J. Nutr. Biochem.* **2013**, *24*, 680–687. [CrossRef]
15. Selvendiran, K.; Singh JP, V.; Krishnan, K.B. Cytoprotective effect of piperine against benzo[a]pyrene induced lung cancer with reference to lipid peroxidation and antioxidant system in Swiss albino mice. *Fitoterapia* **2003**, *74*, 109–115. [CrossRef]
16. Quilaqueo, M.; Millao, S.; Luzardo-Ocampo, I. Inclusion of piperine in β-cyclodextrin complexes improves their bioaccessibility and in vitro antioxidant capacity. *Food Hydrocoll.* **2019**, *91*, 143–152. [CrossRef]
17. He, H.; Zhang, Q.; Wang, J.R. Structure, physicochemical properties and pharmacokinetics of resveratrol and piperine cocrystals. *Crystengcomm* **2017**, *19*, 6154–6163. [CrossRef]
18. Gu, W.; Liu, Y. Characterization and stability of beta-acids/hydroxypropyl-β-cyclodextrin inclusion complex. *J. Mol. Struct.* **2020**, *1201*, 127159. [CrossRef]
19. Hsu, C.M.; Yu, S.C.; Tsai, F.J. Enhancement of rhubarb extract solubility and bioactivity by 2-hydroxypropyl-beta-cyclodextrin. *Carbohydr. Polym.* **2013**, *98*, 1422–1429. [CrossRef]
20. Loftsson, T.; Hreinsdottir, D.; Masson, M. Evaluation of cyclodextrin solubilization of drugs. *Int. J. Pharm.* **2005**, *302*, 18–28. [CrossRef]
21. Loftsson, T.; Brewster, M.E. Pharmaceutical applications of cyclodextrins: Basic science and product development. *J. Pharm. Pharmacol.* **2010**, *62*, 1607–1621. [CrossRef] [PubMed]
22. Ol'khovich, M.; Sharapova, A.; Blokhina, S. A study of the inclusion complex of bioactive thiadiazole derivative with 2-hydroxypropyl-β-cyclodextrin: Preparation, characterization and physicochemical properties. *J. Mol. Liq.* **2019**, *273*, 653–662. [CrossRef]
23. Jovanović, M.; Ćujić-Nikolić, N.; Drinić, Z. Spray drying of Gentiana asclepiadea L. root extract: Successful encapsulation into powders with preserved stability of bioactive compounds. *Ind. Crops Prod.* **2021**, *172*, 114044. [CrossRef]
24. Wolska, E. Fine powder of lipid microparticles—Spray drying process development and optimization. *J. Drug. Del. Sci. Tec.* **2021**, *64*, 102640. [CrossRef]
25. Kurangi, B.; Jalalpure, S.; Jagwani, S. A validated stability-indicating HPLC method for simultaneous estimation of resveratrol and piperine in cubosome and human plasma. *J. Chromatogr. B* **2019**, *1122–1123*, 39–48. [CrossRef] [PubMed]
26. Higuchi, T.K.; Connors, K.A. Phase Solubility Techniques. *Adv. Anal. Chem. Instrum.* **1965**, *4*, 117–212.
27. Wei, Y.; Zhang, J.; Memon, A.H. Molecular model and in vitro antioxidant activity of a water-soluble and stable phloretin/hydroxypropyl-β-cyclodextrin inclusion complex. *J. Mol. Liq.* **2017**, *236*, 68–75. [CrossRef]
28. Roberta, R.N.; Anna, P.; Ananth, P. Cathering. Antioxidant activity applying an improved ABTS radical cation decolorization activity assay. *Free Radic. Biol. Med.* **1999**, *26*, 1231–1237.

29. Martínez-Alonso, S.A.; Carlos, B.D. Encapsulation and solubilization of the antioxidants gallic acid and ethyl, propyl and butyl gallate with β-cyclodextrin. *J. Mol. Liq.* **2015**, *210*, 143–150. [CrossRef]

30. Marques, H.M.C. A review on cyclodextrin encapsulation of essential oils and volatiles. *Flavour. Frag. J.* **2010**, *25*, 313–326. [CrossRef]

31. Shah, A.A.; Shah, A.; Lewis, S.; Ghate, V.; Saklani, R.; Kalkura, N.; Singh, P.K.; Nayak, Y.; Chourasia, M.K. Cyclodextrin based bone regenerative inclusion complex for resveratrol in postmenopausal osteoporosis. *Eur. J. Pharm. Biopharm.* **2021**, *167*, 127–139. [CrossRef] [PubMed]

32. Hao, X.; Sun, X.; Zhu, H.; Xie, L. Hydroxypropyl-β-Cyclodextrin-Complexed Resveratrol Enhanced Antitumor Activity in a Cervical Cancer Model: In Vivo Analysis. *Front. Pharmacol.* **2021**, *12*, 573909. [CrossRef]

33. Stasiłowicz, A.A. Combinations of Piperine with Hydroxypropyl-β-Cyclodextrin as a Multifunctional System. *Int. J. Mol. Sci.* **2021**, *18*, 4195. [CrossRef] [PubMed]

34. Wang, J. Physicochemical and release characterisation of garlic oil-β-cyclodextrin inclusion complexes. *Food Chem.* **2011**, *127*, 1680–1685. [CrossRef]

35. Li, J.; Geng, S.; Wang, Y. The interaction mechanism of oligopeptides containing aromatic rings with beta-cyclodextrin and its derivatives. *Food Chem.* **2019**, *286*, 441–448. [CrossRef]